Dynamic Estimation of Vital Signs with mm-wave FMCW Radar

Su, Guigeng; Petrov, Nikita; Yarovoy, Alexander

DOI
10.1109/EuRAD48048.2021.00060

Publication date
2021

Document Version
Final published version

Published in
EuRAD 2020 - 2020 17th European Radar Conference

Dynamic Estimation of Vital Signs with mm-wave FMCW Radar

Guigeng Su[1], Nikita Petrov[2], Alexander Yarovoy[3]
Microwave Sensing, Signals and Systems (MS3), Delft University of Technology, the Netherlands
{[1]SuGuigeng1994@163.com, [2]N.Petrov@tudelft.nl, [3]A.Yarovoy@tudelft.nl}

***Abstract* — In this paper, we propose a method for continuous monitoring of vital signs — in particular, respiration frequency — with a commercial mm-wave radar. The nearly constant frequency (NCF) model is adopted to represent chest displacement due to respiration and simulate radar response. Based on this model, an extended Kalman filter (EKF) based estimator is developed to track the breathing frequency of a person. The impact of dynamic model parameters is investigated in numerical simulation. The possibility to track breathing frequency with the proposed method is demonstrated by experimental data processing.**

***Keywords* — Vital signs, sequential estimation, extended Kalman filter (EKF).**

I. Introduction

Monitoring the human body's vital (life-sustaining) functions is of prime interest in health care, smart houses, security, and other applications [1]. The standard tools for vital signs monitoring — electrocardiography (ECG) and photoplethysmography (PPG) — require connection to the body and thus limit personal mobility and can not be applied for injured patients (e.g. burned skin, sudden infant death syndrome (SIDS) [2]) and non-cooperative elderly people. Modern contact-less tools for vital signs monitoring are based on radar technologies and benefit from the propagation of microwaves through the clothes. Radar can monitor vital signs by measuring the periodic motion of the human chest caused by the cardiopulmonary activity.

To detect and estimate the parameters of the chest movement, range displacement of the body is measured with an ultra-wideband radar e.g. [3], or induced Doppler frequency shift is measured by a continuous-wave radar, e.g. [4]. Recently, the application of mm-wave (60 GHz and 77 GHz bands) frequency modulated continuous wave (FMCW) radars to vital signs monitoring has been widely investigated. Such radars benefit from the high Doppler sensitivity, required for reliable vital signs detection and monitoring. The penetration depth into human skin was estimated to 1 mm at most with 60 GHz radar [5], which simplifies the analysis of the reflected signal; it was also demonstrated that measured chest movement contains information about both respiration and heartbeat. Good agreement of the respiration movements detected by 80 GHz FMCW radar with reference contact measurements has been shown in [6]. Application of range compression and beam-forming for vital signs monitoring of multiple persons was demonstrated in [7] and further extended to 3D localization in [8].

Extraction of breathing and heartbeat frequencies from radar data is typically based on frequency peak searching in the Doppler power spectrum of the received signal and/or its phase history. Recently, vital sign extraction with empirical mode decomposition and independent component analysis has been investigated [9], [10]. The methods mentioned above are implemented via batch data processing over a long observation time (typically from 10 s to a minute). At the same time, continuous information about a person's state is required in some applications due to the necessity of rapid reaction of the monitoring system to the changes in human body behavior. In this study, we investigate the feasibility of performing the dynamic estimation of the breathing frequency (as the dominant component in the chest movement) with mm-wave radar and propose a Kalman filter-based approach to solve this problem.

The rest of this paper is organized as follows. A nearly constant frequency (NCF) model for periodic processes is adopted for vital signs modeling in Section II. Kalman filter for dynamic estimation of chest movement due to breathing is derived in Section III. Simulation results are presented in Section IV and experimental validation is given in Section V. Finally, conclusions are drawn in Section VI.

II. Data Model

Assume a mm-wave radar transmits a periodic waveform and illuminates a person from the front. The signal reflected from the chest and impinging the radar has a dominant component corresponding to the reflection from the skin due to the low penetration of microwaves into the body [5]. The reflected signal encompasses information about vital signs by measuring the quasi-periodical movement of prothorax and chest cavity, induced by the lung volume changes and the heart-beat. Aiming at the range cell with the strongest reflection and neglecting Doppler effect within a pulse, the received replica of the n-th sweep (or pulse) is given by:

$$y[n] = h[n]e^{j\phi[n]}e^{j2\pi f_c \frac{2R_r[n]}{c}} + u[n], \qquad (1)$$

where $n = 0, \ldots, N-1$ is the slow-time index, $h[n]e^{j\phi[n]}$ is a complex back-scattering coefficient of the body (including the propagation and processing constants with no loss of generality) sampled with pulse repetition interval (PRI) T_r at times $t = nT_r$, $R[n]$ describes the displacement of the chest in radial direction from the radar, and $u[n]$ is an additive noise.

2020 17th European Radar Conference (EuRAD) | 978-2-87487-061-3/21/$31.00 ©2021 IEEE | DOI: 10.23919/EuRAD48048.2021.00060

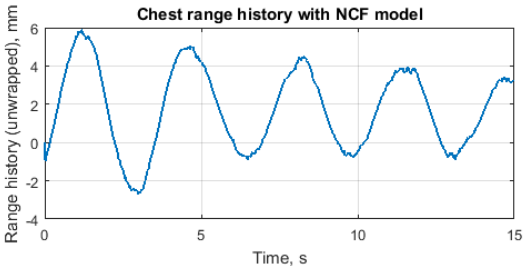

Fig. 1. A range history generated with a nearly constant frequency model

The range history of the chest $R(t)$ is a linear combination of two periodical activities - breathing and heart beat with the prothorax displacement due to breathing with frequency $f_b \in [0.1, 0.4]$ Hz and magnitude $\alpha_b \in [3, 11]$ mm and $f_h \in [1, 2]$ Hz and $\alpha_b \in [0.3, 0.8]$ mm for the heart beat accordingly [11]. Recall that diaphragm displacement due to each of the aforementioned vital signs has sinusoidal like movement (e.g. [12]), and therefore its parameters are typically estimated via the peaks in the Fourier spectrum of the measured range history [13]. It implies that the range history of the chest due to respiration can be modeled with a time-varying sinusoidal:

$$R_r[n] = \alpha[n] \sin\left(2\pi f_b[n] T_r n + \varphi_r\right) + w[n], \qquad (2)$$

where $\alpha[n]$ and $f_b[n]$ are slowly varying respiratory amplitude and frequency, φ_r is the initial phase of respiration and $w[n]$ is a random component, which can also represent the impact of the heartbeat.

A. Dynamic models for periodic signals

The range history (2) of the breathing has the form of a time-varying sinusoid. Dynamic estimation of single-tone frequency and amplitude has been recently addressed in [14]. In this study, we adopt a nearly constant frequency (NCF) dynamic model from [14] for chest movement due to breathing and use it hereinafter for tracking vital signs parameters. The choice of NCF model is determined by its superior performance compared to the other models when the frequency varies slowly [14], the case expected for healthy person respiration.

NCF model is applied directly to the signal (2) by defining new variables: time-varying angular frequency $\omega[n] = 2\pi f_b[n]$, angle $\theta[n]$ and using Taylor series expansion of $\theta[n] = \omega[n] T_r n + \varphi_r$:

$$\begin{aligned} \theta[n] &= \theta[n-1] + T_r \omega[n-1] + \frac{T_r^2}{2} \frac{\partial \omega(t)}{\partial t}\bigg|_{t=(n-1)T_r} \\ \omega[n] &= \omega[n-1] + T_r \frac{\partial \omega(t)}{\partial t}\bigg|_{t=(n-1)T_r} \end{aligned} \qquad (3)$$

and assuming that breathing frequency has small variation over time modeled by $\frac{\partial \omega_t}{\partial t}|_{t=(n-1)T_r} = w_\omega \sim \mathcal{N}(0, \sigma_\omega^2)$. The other unknowns encompassed in the data model (1) and (2) are the magnitude of chest variation $\alpha_r[n]$ and complex back-scattering coefficient $h[n]e^{j\phi[n]}$ are assumed slowly varying processes. An example of the range history generated by NCF model with $\sigma_f = \sigma_\omega/(2\pi) = 0.1$ Hz/s and $\sigma_\alpha = 0.1$ mm/s is shown in Fig. 1.

III. Dynamic Estimation of Vital Signs Parameters

In this section, we propose Kalman filter based dynamic estimation of breathing parameters (frequency and magnitude of chest displacement) from the unwrapped phase history of the received data (1). The corresponding dynamic and observation models are introduced and then the general form of EKF is given.

A. Phase history dynamic model

Since the vital signs information is contained in the phase term in (1), the estimation process can be simplified by processing the phase history (1) directly. However, estimation of frequency f_r and amplitude α_r requires unwrapping of the phase history from the baseband signal. Note that due to the unwrapping process, the unwrapped phase history generally has a non-zero mean (see Fig. 1), considered here by additional unknown parameter $\psi[n]$. Thus, the measurement model is:

$$\begin{aligned} z[n] &= \mathbf{g}(\mathbf{s}[n]) + u[n] \\ &= P\alpha[n] \sin(\theta[n]) + \psi[n] + u[n], \end{aligned} \qquad (4)$$

where $P = 4\pi f_c/c$, the state vector: $\mathbf{s}[n] = [\theta[n], \omega[n], \alpha[n], \psi[n]]^T$ and $u[n] \sim \mathcal{N}\left(0, \sigma_u^2\right)$. For moderate and high SNR of the received signal, the noise of the extracted phase is Gaussian. The Jacobian corresponding to the linearized measurement model can be written by:

$$\mathbf{G}[n] = \begin{bmatrix} P\alpha\cos(\theta) & 0 & P\sin(\theta) & 1 \end{bmatrix}\Big|_{\mathbf{s}=\hat{\mathbf{s}}[n|n-1]}. \qquad (5)$$

For unwrapped phase history observation, the dynamics of NCF model is given by:

$$\begin{aligned} \mathbf{s}[n] &= \mathbf{A}\mathbf{s}[n-1] + \mathbf{B}\mathbf{v}[n] \\ &= \begin{bmatrix} 1 & T_r & 0 & 0 \\ 0 & 1 & 0 & 0 \\ 0 & 0 & 1 & 0 \\ 0 & 0 & 0 & 1 \end{bmatrix} \mathbf{s}[n-1] + \begin{bmatrix} T_r^2/2 & 0 & 0 \\ T_r & 0 & 0 \\ 0 & T_r & 0 \\ 0 & 0 & 1 \end{bmatrix} \tilde{\mathbf{v}}[n], \end{aligned} \qquad (6)$$

where $\mathbf{v}_[n] = [v_\omega[n], v_\alpha[n], v_\psi[n]]^T$ is Gaussian driving noise: $\mathbf{v}[n] \sim \mathcal{N}(\mathbf{0}_{3\times 1}, \tilde{\mathbf{Q}})$ with $\tilde{\mathbf{Q}} = E\left\{\mathbf{v}[n]\mathbf{v}^T[n]\right\} = \mathrm{diag}\{\sigma_\omega^2, \sigma_\alpha^2, \sigma_\psi^2\}$.

B. Burst processing

The dynamic estimator based on the aforementioned model operates well if the estimated parameters are initialized in the vicinity of the true values. In the absence of prior knowledge about these parameters, the estimators can diverge. To alleviate this problem, we propose to apply a Kalman filter to overlapping bursts of data containing L samples. It implies the modification of the measurement model (4) for $l = 0, \ldots, L-1$ via:

$$\begin{aligned} \bar{\mathbf{z}}[n] &= \bar{\mathbf{g}}(\mathbf{s}[n]) + \bar{\mathbf{u}}[n] \\ &= \begin{bmatrix} P\alpha[n]\sin(\theta[n]) + \phi[n] \\ P\alpha[n]\sin(\theta[n] + T_r) + \phi[n] \\ \cdots \\ P\alpha[n]\sin(\theta[n] + (L-1)T_r) + \phi[n] \end{bmatrix} + \bar{\mathbf{u}}[n], \end{aligned} \qquad (7)$$

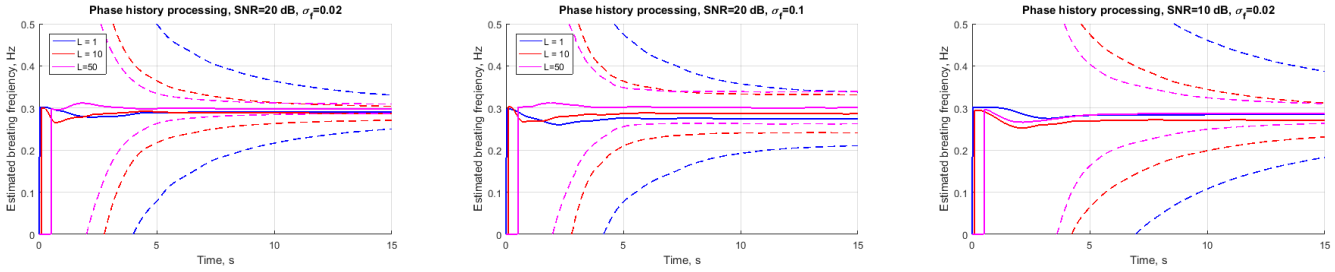

Fig. 2. Breathing frequency estimation with $\pm\sigma_f$ bounds using unwrapped phase history, $\sigma_\alpha = 0.5$ mm/s, $\sigma_\psi = 10^{-6}$ 1/s: *a* - σ_f= 0.02 Hz/s, SNR=20 dB; *b* - σ_f= 0.1 Hz/s, SNR=20 dB; *c* - σ_f= 0.02 Hz/s, SNR=10 dB

The measurement noise is assumed white Gaussian with $\bar{\mathbf{R}} = E\left\{\bar{\mathbf{u}}[n]\bar{\mathbf{u}}^T[n]\right\} = \sigma_u^2\mathbf{I}_L$. A few comments should be made on (7). First, it assumes no dynamics of the process over the duration of the burst. This is a reasonable assumption for a slow-moving person. Second, the assumption of noise independence in the adjacent bursts is rigorously not correct if they are overlapping. However, the same simplification is commonly made in spectrum analysis to design efficient estimators, see e.g. [15].

C. Extended Kalman Filter (EKF)

To solve the breathing frequency estimation problem we propose to use a Kalman filter, selected for its simplicity and efficient implementation. Because of the non-linear measurement model, extended Kalman filter (EKF) [16] is considered. Moreover, in this paper we focus on the sequential estimation of the breathing frequency only; thus more appropriate signal models (including the impact of heartbeat) and more advanced and robust solutions (e.g. particle filtering) are out of the scope of this paper.

The dynamic estimation of the breathing parameters is performed by EKF, which consists of two steps. First, the prediction step is based on dynamic model (6):

$$\begin{aligned}\hat{\mathbf{s}}[n|n-1] &= \mathbf{A}\hat{\mathbf{s}}[n-1|n-1];\\ \mathbf{M}[n|n-1] &= \mathbf{A}\mathbf{M}[n-1|n-1]\mathbf{A}^T + \mathbf{B}\mathbf{Q}\mathbf{B}^T,\end{aligned} \tag{8}$$

where $\hat{\mathbf{s}}[n|n-1]$ denotes the prediction of the state obtained at step $n-1$ and $\hat{\mathbf{s}}[n-1|n-1]$ stands for its estimation. Minimum prediction mean squared error (MSE) matrix is denoted by $\mathbf{M}$.

Second, the correction step is based on the measurement model:

$$\begin{aligned}\mathbf{K}[n] &= \mathbf{M}[n|n-1]\mathbf{G}^T[n]\left(\mathbf{R} + \mathbf{G}[n]\mathbf{M}[n|n-1]\mathbf{G}^T[n]\right);\\ \hat{\mathbf{s}}[n|n] &= \hat{\mathbf{s}}[n|n-1] + \mathbf{K}[n]\left(\mathbf{z}[n] - \mathbf{g}(\hat{\mathbf{s}}[n|n-1])\right);\\ \mathbf{M}[n|n] &= \left(\mathbf{I}_4 - \mathbf{K}[n]\mathbf{G}[n]\right)\mathbf{M}[n|n-1],\end{aligned} \tag{9}$$

where $\mathbf{K}[n]$ is a Kalman gain matrix.

Note that due to the linear approximation of the non-linear measurement process, the convergence of EKF can not be guaranteed. That implies the need for reasonable initialization of all the parameters for reliable dynamic estimation. This problem is investigated in the next section. Moreover, there are no constraints for the EKF estimation on the value of angular frequency ω and amplitude α; therefore both frequency and amplitude estimations can be negative. This brings the ambiguity of the estimated values: with no constraints on realistic parameters, there exist a few combinations of ω, α, ϕ which can represent the same signal. However, these sets of parameters have equal absolute values of frequency and amplitude $|\omega|, |\alpha|$, which, therefore, are considered for performance assessment hereinafter.

IV. Simulations

The following radar parameters are fixed in the simulations: $f_c = 77$ GHz, pulse repetition frequency (PRF): $F_r = 100$ Hz and total observation time is 15 s. The standard phase unwrapping processing is applied for phase history extraction from complex data.

The simulated signal has the following values for: $f_b[0] = 0.3$ Hz, $\alpha[0] = 4$ mm and follows NCF model with $\sigma_a = 0.1$ mm/s, $\sigma_\psi = 10^{-3}$ and $\sigma_f = 0.02$ Hz/s if not mentioned otherwise. The initialization of the filter is made by $\hat{\mathbf{s}}[0|0] = \left[0, 2\pi\mathcal{N}(0.25, 0.05^2), \mathcal{N}\left(4\cdot10^{-3}, (\cdot10^{-3})^2\right), 0\right]^T$ to cover possible error of the estimated parameters at the initialization. To account for the estimation error at the initialization, the MMSE matrix is initialized with $\mathbf{M}[0|0] = \mathrm{diag}\left((3\pi)^2, (2\pi\cdot0.3)^2, (3\cdot10^{-3})^2, (10^{-2})^2\right)$.

The simulation results are presented in Fig. 2. Each plot demonstrates averaged over 100 Monte-Carlo trials estimated breating frequency $E\{\hat{f}_b[n|n]\}$ bounded by $\sqrt{E\{\mathbf{M}_{2,2}[n|n]\}}$. We refer to SNR per pulse before unwrapping process.

Simulation results for SNR=20 dB and $\sigma_f = 0.02$ Hz/s are shown in Fig. 2, a. The curves of different colors correspond to different filter lengths, namely $L = \{1, 10, 50\}$. The filter with no burst processing ($L = 1$) has larger variance as the result of divergence in some scenarios, primarily because of ambiguities in amplitude and phase estimation. We have noticed that the phase error at the initialization has a major impact on the convergence. This uncertainty is sufficiently reduced by applying a filter with $L = \{10, 50\}$. Fig. 2, b shows the results for larger frequency variation. In the demonstrated scenarios, the filters with $L = \{10, 50\}$ converge to the uncertainty determined by the dynamic model. The results for SNR=10 dB, presented in Fig. 2, c shows the increased uncertainty of the

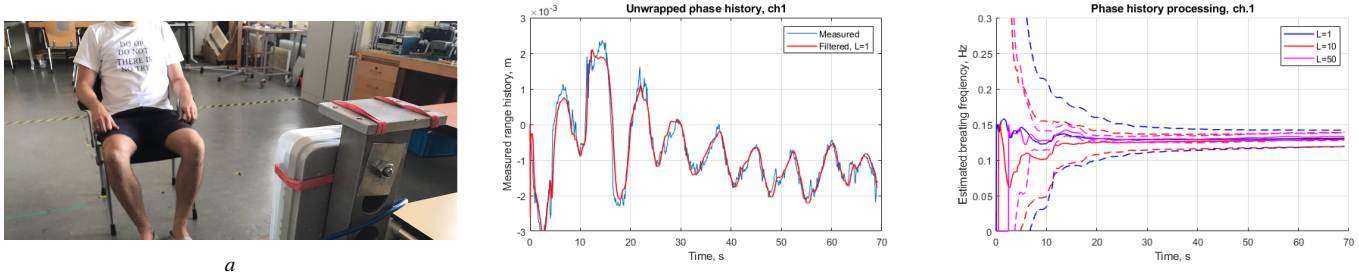

a *b* *c*

Fig. 3. *a* - Measurement scenario; *b* - Measured and filtered phase history; *c* - Estimated breathing frequency.

estimation due to lower SNR and larger errors of unwrapping pre-processing.

V. Experimental Analysis

The proposed estimation technique has been validated by applying to a real data set collected with a commercial FMCW radar operating at $f_c = 77$ GHz frequency band with a bandwidth $B = 1GHz$ and $F_r \approx 20$ Hz. The person was sitting about 2 m away from the radar as shown in Fig. 3, a.

Phase history demonstrated in Fig. 3, b is extracted from slow-time data in the range cell with the strongest response. The dynamic model in this case was set to: $\sigma_\omega = 2\pi \cdot 0.003$ Hz, $\sigma_\alpha = 10^{-3}$ mm, $\sigma_\phi = 10^{-3}$. To stabilize the convergence and minimize the impact of the heartbeat on the algorithm convergence, the variance of the measurement noise in $\mathbf{R}$ was set 10 dB above the measured noise floor. In Fig. 3, b, the predicted signal $z[n] = \mathbf{g}(\mathbf{s}[n])$ is demonstrated and it agrees well with the data already in a few seconds. The breathing frequency estimation with $L = \{1, 10, 50\}$, shown on Fig.3, c, converges to $f_b \approx 0.14$ Hz and agrees well with the spectrogramm of the range hitory (not shown here). This example demonstrates the possibility to perform continuos tracking of the breathing frequency with the proposed method.

VI. Conclusion

For the first time, remote monitoring of the vital signs has been formulated as a dynamic estimation problem of the breathing frequency with mm-wave radar. A nearly-constant frequency (NCF) model has been proposed to model the displacement of the chest due to breathing with sufficient for the application fidelity. Based on the NCF model, an extended Kalman filter for breathing frequency estimation was developed. Simulation results and experimental data analysis have demonstrated that with a reasonable initialization, the proposed method can provide accurate and up-to-date information about human breathing already after collecting a few seconds of raw data.

References

[1] J. Lin and C. Li, "Wireless non-contact detection of heartbeat and respiration using low-power microwave radar sensor," in *2007 Asia-Pacific Microwave Conference*. IEEE, 2007, pp. 1–4.

[2] H. Forster, O. Ipsiroglu, R. Kerbl, and E. Paditz, "Sudden infant death and pediatric sleep disorders," 2003.

[3] A. Yarovoy, L. Ligthart, J. Matuzas, and B. Levitas, "Uwb radar for human being detection," *IEEE Aerospace and Electronic Systems Magazine*, vol. 21, no. 3, pp. 10–14, 2006.

[4] C. Li, J. Lin, and Y. Xiao, "Robust overnight monitoring of human vital signs by a non-contact respiration and heartbeat detector," in *2006 International Conference of the IEEE Engineering in Medicine and Biology Society*. IEEE, 2006, pp. 2235–2238.

[5] T. Wu, T. S. Rappaport, and C. M. Collins, "The human body and millimeter-wave wireless communication systems: Interactions and implications," in *2015 IEEE International Conference on Communications (ICC)*, June 2015, pp. 2423–2429.

[6] S. Wang, A. Pohl, T. Jaeschke, M. Czaplik, M. Köny, S. Leonhardt, and N. Pohl, "A novel ultra-wideband 80 GHz FMCW radar system for contactless monitoring of vital signs," in *2015 37th Annual International Conference of the IEEE Engineering in Medicine and Biology Society (EMBC)*, Aug 2015, pp. 4978–4981.

[7] A. Ahmad, J. C. Roh, D. Wang, and A. Dubey, "Vital signs monitoring of multiple people using a fmcw millimeter-wave sensor," in *2018 IEEE Radar Conference (RadarConf18)*, April 2018, pp. 1450–1455.

[8] S. Wang, S. Kueppers, H. Cetinkaya, and R. Herschel, "3d localization and vital sign detection of human subjects with a 120 ghz mimo radar," in *2019 20th International Radar Symposium (IRS)*, June 2019, pp. 1–6.

[9] F. Weishaupt, I. Walterscheid, O. Biallawons, and J. Klare, "Vital sign localization and measurement using an lfmcw mimo radar," in *2018 19th International Radar Symposium (IRS)*, June 2018, pp. 1–8.

[10] M. Mercuri, Y.-H. Liu, I. Lorato, T. Torfs, F. Wieringa, A. Bourdoux, and C. Van Hoof, "A direct phase-tracking doppler radar using wavelet independent component analysis for non-contact respiratory and heart rate monitoring," *IEEE transactions on biomedical circuits and systems*, vol. 12, no. 3, pp. 632–643, 2018.

[11] K. Konno and J. Mead, "Measurement of the separate volume changes of rib cage and abdomen during breathing," *Journal of applied physiology*, vol. 22, no. 3, pp. 407–422, 1967.

[12] R. C. Veltkamp and B. Piest, "A physiological torso model for realistic breathing simulation," in *3D Physiological Human Workshop*. Springer, 2009, pp. 84–94.

[13] M.-C. Huang, J. J. Liu, W. Xu, C. Gu, C. Li, and M. Sarrafzadeh, "A self-calibrating radar sensor system for measuring vital signs," *IEEE transactions on biomedical circuits and systems*, vol. 10, no. 2, pp. 352–363, 2015.

[14] W. Ng, C. Ji, W. Ma, and H. C. So, "A study on particle filters for single-tone frequency tracking," *IEEE Transactions on Aerospace and Electronic Systems*, vol. 45, no. 3, pp. 1111–1125, 2009.

[15] J. Li and P. Stoica, "An adaptive filtering approach to spectral estimation and sar imaging," *IEEE Transactions on Signal Processing*, vol. 44, no. 6, pp. 1469–1484, 1996.

[16] S. M. Kay, *Fundamentals of Statistical Signal Processing: Estimation Theory*. Prentice Hall PTR, 1993.